

Enhancing up conversion luminescence effect of β -NaYF₄: Yb³⁺ and Tm³⁺ by Li⁺ ion doped approach

Min-Hua Tsai¹ · Tin-Wei Shen¹ · Kuan-Bo Lin¹ · Yen-Hsun Su¹

Received: 10 April 2017 / Accepted: 10 October 2017 / Published online: 31 October 2017
© Springer Science+Business Media, LLC 2017

Abstract Up-conversion (UC) is a photoluminescence process which converts few low energy photons to a higher energy photon. This process has more potential usages in many different fields like bioimaging, solar spectrum tuning, and security encoding. Nowadays, researches about UC mostly focusing on biomedical signory and synthesis of nanoparticles. The synthesis of NaYF₄ nanoparticles executed under series of pH value condition results in different morphology and photoluminescence effect. Samples in low pH value created better consequent and quality than the specimen which had higher pH value. In addition, we observed NaYF₄ samples of doping Li⁺, realizing that the action of distorting in the local symmetry around rare-earth ions is caused by Li⁺ doping. The NaYF₄ microparticles which doped higher concentration of Li⁺ has strong fluorescence properties and intensities compared with their corresponding group of Li⁺-free, the blue emission 479 nm luminescence intensities and 454 nm luminescence intensities in NaYF₄:Yb³⁺, Tm³⁺ microparticles doped 20 mol% Li⁺ are enhanced 3 and 8 times, separately. And violet emission luminescence intensities around 345 and 360 nm are about 10 and 7 times, respectively. The result indicated that the improved UC luminescence of NaYF₄:Yb³⁺, Tm³⁺ microparticles with Li⁺ doping have potentially applications.

Keywords Up-conversion · NaYF₄ · Hydrothermal synthesis · Doping ion · pH value modified

This article is part of the Topical Collection on Photonic Science and Engineering on the Micro/Nano Scale.

Guest edited by Yen-Hsun Su, Lei Liu, Yiting Yu and Yikun Liu.

✉ Yen-Hsun Su
yhsu@mail.ncku.edu.tw
Min-Hua Tsai
e44006092@gmail.com

¹ Department of Materials Science and Engineering, National Cheng Kung University, 701 No. 1, University Rd, Tainan, Taiwan

1 Introduction

Since more than a decade ago, people put numerous attention on up-conversion (UC) luminescence of lanthanide-doped materials, On account of their distinct luminescent behaviors and the ability to convert near infrared radiations into visible radiations in nonlinear optical process, which showed great potential in many fields applications such as biomedical imaging, drug delivery, laser source, photocatalyst and solar energy harvesting (Cao et al. 2010; Chatti et al. 2016; Cheng et al. 2011, 2013; Gauthier et al. 2013; Gnanasammandhan et al. 2016; Li et al. 2015, 2016; Liu et al. 2013, 2016a; Wu et al. 2015; Zhou et al. 2012).

The visible light and the energy in the near-infrared (NIR) range commonly only be used by the sensitizers of solar cells because the bandgap of thin film was large, The appearance implies the semiconductor only can absorb the light which wavelength shorter than 700 nm. This phenomenon express large-scope solar spectrum cannot be absorbed, specifically near-infrared light. The phenomenon also is called transmission losses. The appearance mean that the wasted situation of solar energy is almost nearly half of whole energy (Wang et al. 2011). Therefore, the scientists try to access the near-infrared light for solar cells through many methods. Among all the methods, the dopant ions of trivalent lanthanides materials with their up-conversion properties obtained the most attention. This mechanism of the dopant ions is described that the ions absorb two or more the incoming low-energy photons and the other dopants acts as the emitter ions. The emitter ions emit the single and higher-energy photon after the up-conversion process to harvest the near infrared light for solar cells, and then improve the photoelectric conversion efficiency (Shang et al. 2015; Wang et al. 2015).

Reports (Shao et al. 2016) show that the host lattice NaYF₄ has two lattice types, namely cubic structure (also known as α phase), and hexahedron structure (hexagonal phase, also known as β phase), they have dissimilar symmetry and ion substitutional modes. β -NaYF₄ structure belongs to hexagonal crystal orientation, have greater up-conversion efficiency about ten times than the α -NaYF₄ of cubic structure. Thus β -NaYF₄ often be a first choice for up-conversion luminescent materials (Chen et al. 2015). A number of synthetic methods with doped rare earth ion have been proposed by previous researches (Li et al. 2017; Liang et al. 2007; Liu et al. 2016b; Schäfer et al. 2009; Wang et al. 2008; Xiang et al. 2015; Yi and Chow 2006).

In the rare earth ions, 4f electronic transitions are parity forbidden according to the quantum mechanical selection rules. However, when the rare-earth ion situates at low symmetry sites, the forbiddance can be partially broken. Hence, the modification of rare-earth ions' local environment can expectantly enhance their luminescence intensity of materials (Etchart et al. 2011; Nadort et al. 2016; Page et al. 1998; Pollnau et al. 2000; Timofeev et al. 1996; Wu et al. 2016a, b; Yang et al. 2010; Zhang et al. 2015).

The method of doping Li⁺ changing the crystal field symmetry around the rare-earth ions have significantly effect for increasing up-conversion luminescence intensity (Liu et al. 2006). Due to the small Li⁺ cationic radius elements, Li ion is easy to either occupy site substitutionally or interstitially in the host lattice and change the crystal field symmetry around the trivalent lanthanide ions, which influences the increasing the result of emission intensity. For instance, Zhang's group reported 8 and 5 times increase of 452 and 479 nm UC emissions in Li⁺ doped NaYF₄:Yb³⁺, Tm³⁺ nanocrystals (Zhao et al. 2013). And Lin's group improve up-conversion luminescence intensities of blue emission (477 nm) in β -NaYF₄:Yb³⁺, Tm³⁺ microcrystals doped with 15 mol% Li⁺ are enhanced up to 6 times (Lin et al. 2015a). The internalization of lithium ions which doped into up-conversion host

lattice plays an important role in enhancing the luminous intensity. (Dou and Zhang 2011; Wang and Nann 2009; Yin et al. 2012) Li⁺ ions can be simply placed into the NaYF₄ lattice to set the neighboring Rare earth (RE) ions owing to smaller ionic diameters of Li⁺ ions. The doping of Li⁺ do not damage the local structure around the rare earth ions, but only adjust the local symmetry near rare earth ions, so that they are more favorable for photoluminescence.

Here, we provide a solution to increase β -NaYF₄:Yb³⁺, Tm³⁺ luminescence intensity. We realize the pH value has a powerful influence on the successful synthesis result of β -NaYF₄ which is known that has better up-conversion phosphor than α phase. In higher pH value case, α -phase NaYF₄ easily exist in the product, which implies that low productivity. Under low pH value condition, β -NaYF₄ is formed and affects the morphology which relates to the photoluminescence property. Therefore, we will try to dope Li⁺ ions in sample under lower pH environment. This method is more effective to increase the luminescence intensity of the β -NaYF₄:Yb³⁺, Tm³⁺ material.

2 Experimental section

2.1 Materials

All of the chemicals were used without any further purification process. The RE(NO₃)₃ (RE = Y, Yb, Tm, 0.5 M of Y(NO₃)₃, 0.5 M of Yb(NO₃)₃ and 0.5 M of Tm(NO₃)₃) solutions were completed by dissolving the chemicals ($\geq 99\%$) in deionized water at room temperature.

2.2 Synthesis of β -NaYF₄: Yb³⁺, Tm³⁺ microparticles

A modified hydrothermal method took sodium citrate as a chelating agent to synthesize β -NaYF₄ hexagonal crystals with different pH value by adding various amounts of NaOH or HNO₃ in the original liquid. In a typical process, we added 23.8 mmol NaF to a mixed solution which putted into a 20 mmol of sodium citrate and 20 mL of deionized water. Under vigorous stirring for 10 min to made the solution dissolve completely. Subsequently, 1.56 mmol of Y(NO₃)₃ (1 M, 1.56 mL), 0.4 mmol of Yb(NO₃)₃ (1 M, 0.4 mL) and 0.04 mmol of Tm(NO₃)₃ (1 M, 0.04 mL) were added into the above solution to form a obvious colloidal suspension and kept stirring for another 30 min, then put different capacity of 1 M NaOH or HNO₃ in the liquid to adjust the pH value. Finally, the resulting mixture was transferred into a 50 mL stainless Teflon-lined autoclave, which was sealed and heated at 200 °C for 24 h in an electric drying oven. The reaction mixture was centrifuged for 20 min at a speed of 4000 rpm, the precipitate was washed with deionized water several times and dried at 80 °C overnight.

2.3 Synthesis of β -NaYF₄: Yb³⁺, Tm³⁺ microparticles with Li⁺ doped

Li⁺ co-doped NaYF₄:Yb³⁺, Tm³⁺ microparticles also were synthesized by a simple hydrothermal procedure. In a typical process, we added 23.8 – x mmol NaF to a mixed solution which putted into a 20 mmol of sodium citrate and 20 mL of deionized water. The solution was under vigorous stirring for 10 min to dissolve uniformly. Subsequently, 1.56 mmol of Y(NO₃)₃ (1 M, 1.56 mL), 0.4 mmol of Yb(NO₃)₃ (1 M, 0.4 mL) and

0.04 mmol of $\text{Tm}(\text{NO}_3)_3$ (1 M, 0.04 mL) were added into the above solution to form a obvious colloidal suspension and kept stirring for another 30 min. At this time, x mmol LiNO_3 (0.5 M, $2 \times \text{mL}$), $x/2$ mmol NH_4HF_2 (1 M, $x/2 \text{ mL}$) and 15 mL deionized water were mixed together and uniformly stirred for another 30 min to become a clarified uniform solution, then put different capacity of 1 M HNO_3 in the liquid to adjust the pH value to four. Finally, the resulting mixture was transferred into a 50 mL stainless Teflon-lined autoclave, which was sealed and heated at 200 °C for 24 h in an electric drying oven. The reaction mixture was centrifuged for 20 min at a speed of 4000 rpm, the precipitate was washed with deionized water several times and dried at 80 °C overnight.

2.4 Characterization

The crystal structures of the samples were determined using an X-ray diffractometer Miniflex from Rigaku Company with $\text{CuK}\alpha_{1+2} = 1.54184 \text{ \AA}$ in the 2θ range from 10 to 70. And we used ICCD-PDF of analysis software named Material Data Inc. (MDI) Jade 5.0 to analyzed crystalline phase of powder. The morphologies of the samples were observed by HITACHI SU8000 High-Resolution Field Emission Scanning Electron Microscope (FE-SEM). In this experiment, a self-built system of equipment in our laboratory was used for the photoluminescence spectrum analysis. The up-conversion emission spectra were measured by the spectrometer under the excitation of 980 nm laser ($> 500 \mu\text{W}$ CW Laser) focused one set of focusing mirrors and then processed through the computer software SpectraSuite.

3 Results and discussion

3.1 Phase and morphology

The crystal phase of host lattice as shown in Fig. 1a. The synthesis of $\beta\text{-NaYF}_4$ is successful in our sample with no other impure phase. All the sample of NaYF_4 hexagonal structure, which according to Powder Diffraction File PDF 28-1192. The doping of Li^+ ions did not cause the appearance of other phases. The NaYF_4 sample with lower pH value have the stronger intensity at peak of $2\theta = 29.9^\circ$, which means (110) phase. The weaker intensity is at peak of $2\theta = 30.9^\circ$, which represents (101) phase. The relative ratios of (110) and (001) diffraction peak intensities in the samples were modified by changing the pH of the precursor solution. The results point out when the synthesis of NaYF_4 is in acidic environment, the phase of $\beta\text{-NaYF}_4$ crystal tend to grow along (110) crystal orientation direction. When the synthesis of NaYF_4 is in alkaline solution, the phase of $\beta\text{-NaYF}_4$ crystal tend to grow along (101) crystal orientation direction than (110) crystal orientation direction. This phenomenon which pH value affects the direction of crystal growth is also known from previous studies (Chun-Long et al. 2015). This phenomenon shows that the $\beta\text{-NaYF}_4$ crystal grows along the (110) plane with the increase of pH value. While the orientation growth along the (001) crystal plane is suppressed. The results show that the length-diameter ratio of the samples grown along the (001) and (110) planes becomes smaller as the pH value increases.

X-ray diffraction patterns of 0, 5, 10, 15, and 18 mol% of Li^+ doped $\text{NaYF}_4\text{:Yb}^{3+}$, Tm^{3+} microcrystals where the initial pH value is 4 in synthetic environment (Shown in Fig. 1b. The standard crystalline phase of hexagonal structure (JCPDS 28-1192) are

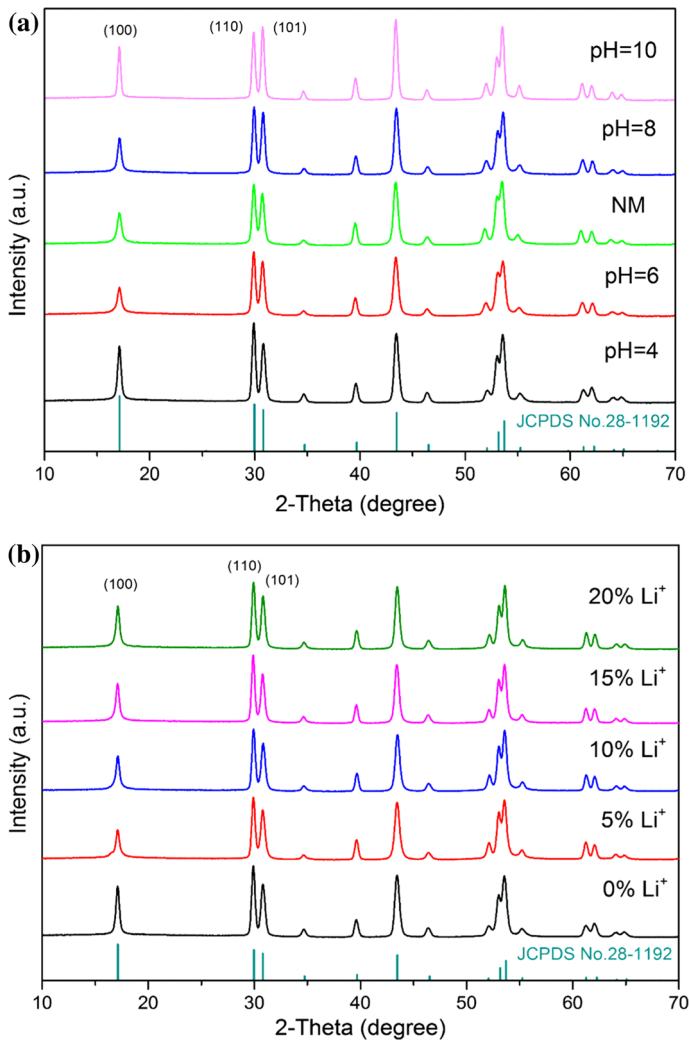


Fig. 1 **a** The XRD patterns of NaYF₄:Yb³⁺, Tm³⁺ microcrystals with different pH value in synthetic environment correspondingly. **b** X-ray diffraction patterns of 0, 5, 10, 15 and 20% Li⁺ doped NaYF₄:Yb³⁺, Tm³⁺ microcrystals. The standard crystalline phase of hexagonal structure (JCPDS 28-1192) are marked by a vertical green lines. (Color figure online)

marked by a vertical green lines in the Fig. 1b. As similar as Fig. 1a, from the patterns, the peak displays that the high purity β -NaYF₄ crystal has been synthesized.

The magnified XRD patterns of 0, 5, 10, 15 and 20 mol% Li⁺ doped NaYF₄:Yb³⁺, Tm³⁺ microcrystals has showed in the Fig. 2, which appears peak offsets at the diffraction angle $2\theta = 29.9^\circ$.

When we observe the peak shift due to the doping of the Li⁺ ion which concentration increases from 0 to 10 mol%, as can be seen clearly, a slight shift of peaks toward larger angles. At the moment when the Li⁺ concentration continuously increases to 15 mol%, the diffraction peak moves reverse direction. After 15 mol% concentration, the peak shifts

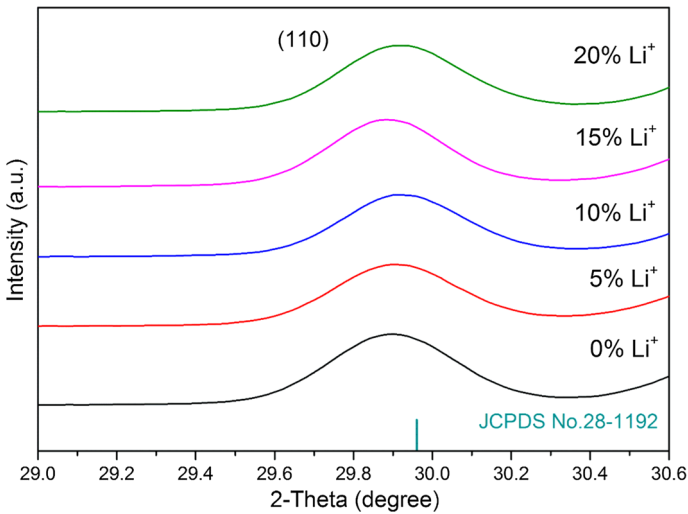


Fig. 2 XRD patterns of 0, 5, 10, 15 and 20 mol% Li^+ doped $\text{NaYF}_4:\text{Yb}^{3+}, \text{Tm}^{3+}$ microcrystals. The magnified insets show peak offsets at the diffraction angle $2\theta = 29.9^\circ$

toward larger angles again. This phenomenon may be caused by the characteristic of slightly smaller ionic radius of Li^+ . Studies have shown the Li^+ ionic radius (0.68 Å) is smaller than that of Na^+ (0.97 Å). Li^+ is small enough to occupy any crystal site, like substituting for the Na^+ ions or interstitial sites or coexist in the two ways (Lin et al. 2015b). When Li^+ has smaller radius than that of Na^+ , the lattice shrinks and inter-planar distance d narrow. According to the Bragg's law: $n\lambda = 2d \sin \theta$, where d is the inter-planar distance of host lattice, θ is the diffraction angle, and λ is the diffraction wavelength. The diffraction angle θ increases, which represents that Li^+ has been placed into the crystal lattice well. On the contrary, Li^+ entering the interstitial sites make the lattice expand. The inter-planar distance of host lattice d increases visibly. The diffraction angle θ shifts toward the lower.

When the concentration of Li^+ is below 10 mol%, the substitution behavior of Li^+ happen to replace Na^+ . Li^+ begins to take interstitial sites with higher 15 mol% concentration. Until Li^+ concentration reach 20 mol%, the substitution behavior of Li^+ appear again.

The SEM images of NaYF_4 under series of pH value condition (4/6/non-modified/8/10) has shown in Fig. 3 with the increase of pH value from 4 to 10. The average particle size of $\text{NaYF}_4:\text{Yb}^{3+}, \text{Tm}^{3+}$ microcrystals are 1.0, 0.75, 0.63, 0.9, and 1.33 μm , respectively. The morphology of NaYF_4 is affected by pH value. The morphologies of the samples with extreme value on both ends are uniform hexagonal micro-prisms. In neutral environment, the NaYF_4 crystal grow to elliptic cylindrical and inconspicuous in shape. Those results express the $\beta\text{-NaYF}_4$ crystal tends to crystallize to hexagonal shape in acidic and alkaline environments, but is not suitable in neutral environment.

3.2 Up-conversion luminescence properties

In order to compare the up-conversion luminescence effect of NaYF_4 sample which were adjusted the pH value in the precursor solution with that of non-modified pH value NaYF_4

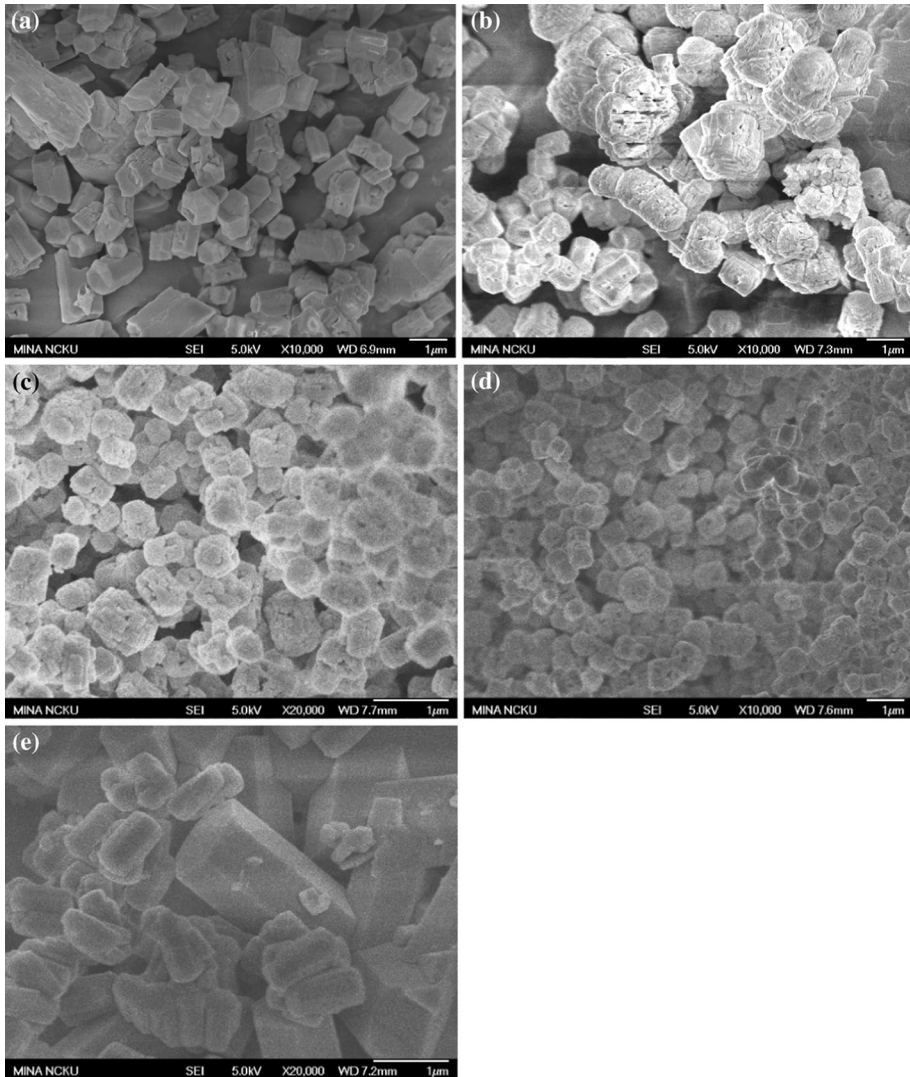


Fig. 3 SEM images of NaYF₄:Yb³⁺, Tm³⁺ microcrystals with different pH value in synthetic environment correspondingly. **a** pH4 sample, **b** pH6 sample, **c** non-modified sample, **d** pH8 sample and **e** pH10 sample

sample, we measured the luminescence intensity of the samples synthesized at different pH values.

Figure 4 display the up-conversion luminescence spectra of NaYF₄:Yb³⁺, Tm³⁺ microcrystals with different pH value in synthetic environment correspondingly under 980 nm excitation with > 500 μ W CW Laser. As shown in Fig. 4, some strong emission peak intensities are observed in the range of 300–850 nm. These emission spectra displays some strong blue emission centered at 479 and 454 nm and red emission centered at 654 nm which corresponding to the electronic transitions of $^1G_4 \rightarrow ^3H_6$, $^1D_2 \rightarrow ^3F_4$ and $^1G_4 \rightarrow ^3F_4$ of Tm³⁺, respectively. In addition there are observed IR emission peak at 796 nm which is form from the transitions of $^3H_4 \rightarrow ^3H_6$.

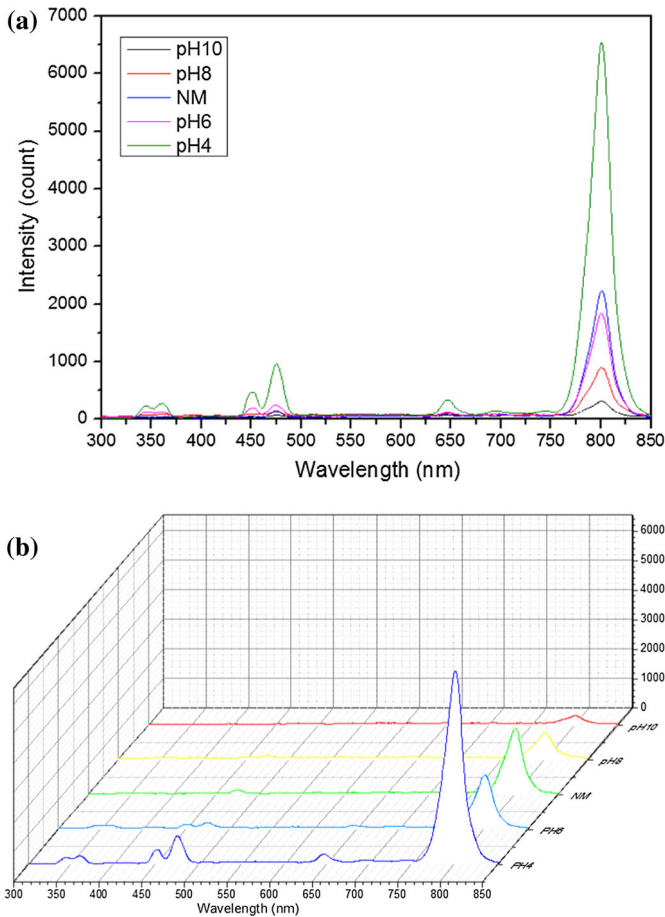


Fig. 4 UC luminescence spectra of **a** $\text{NaYF}_4:\text{Yb}^{3+}, \text{Tm}^{3+}$ microcrystals with different pH value in synthetic environment correspondingly under 980 nm excitation with $> 500 \mu\text{W}$ CW Laser. **b** 3D diagram of different pH value $\text{NaYF}_4:\text{Yb}^{3+}, \text{Tm}^{3+}$ microcrystals under 980 nm excitation

The up-conversion luminescence mechanism is illustrated from the energy-level diagram of $\text{Yb}^{3+}, \text{Tm}^{3+}$ in the $\beta\text{-NaYF}_4$ system with an attentive explanation in Fig. 5. As the figure demonstrates, the blue emission centered at 479 and 454 nm and red emission centered at 654 nm in $\text{NaYF}_4:\text{Yb}^{3+}, \text{Tm}^{3+}$ system are separately three-photon and two-photon processes under 980 nm excitation. Additionally, the IR emission also belongs to two-photon luminescent processes.

From Fig. 4, it is observable that the luminescent intensity is inversely proportional to the initial pH value. When the pH value is lower, the intensity is stronger. Therefore, samples of pH4 have the best up-conversion luminescent properties. The NaYF_4 synthesized under alkaline solution has a decrease in emission intensity. This phenomenon should be caused by the difficult formation of hexagonal phase NaYF_4 under alkaline solution. From the previous literature (Suli et al. 2014; Wu et al. 2013), we know that the sample with high pH value easily produces more cubic phase NaYF_4 when the synthesis reaction time is less than 12 h. The cubic phase NaYF_4 has much lower luminescence efficiency

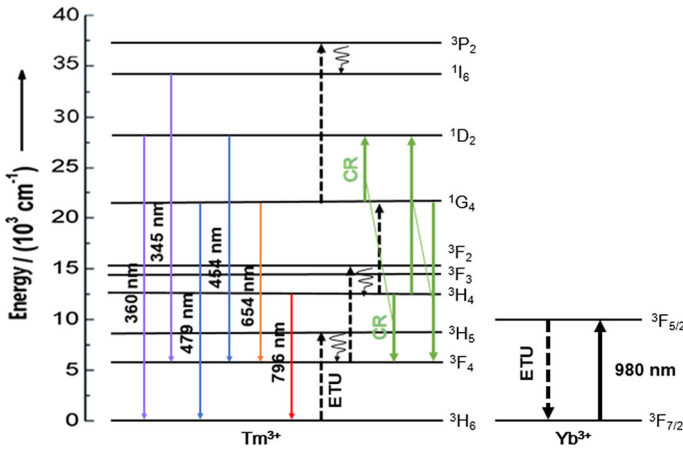


Fig. 5 Simplified energy-level diagrams of Tm³⁺ and Yb³⁺ and the corresponding UC mechanisms. CR is the abbreviation of cross relaxation of Tm³⁺ behavior, and ETU is energy transfer up-conversion

than hexagonal NaYF₄. The appearance explores the effect of pH value on the luminescent properties. The surface quenching effect of hydroxyl groups can give a reasonable explanation. A hydroxyl group having a high absorption peak of phonon energy inactivates the rare earth ions and quenches the emission intensity of NaYF₄ microcrystals. Therefore, NaYF₄: Yb³⁺, Tm³⁺ with favorable luminescence property can be synthesized well under acidic synthesis environment.

The photographs of up-conversion luminescence of NaYF₄:Yb³⁺, Tm³⁺ microcrystals with distinct pH value under 980 nm excitation were seen in Fig. 6. The fluorescence intensity is greatly enhanced in the lower pH value environment, the fluorescence intensity of sample synthesized in acidic condition is evidently observed with the naked eyes, so the up-conversion luminescence in pH4 sample condition is the brightest. This result can be



Fig. 6 Photographs of UC luminescence of **a** pH4 sample, **b** pH6 sample, **c** non-modified sample, **d** pH8 sample and **e** pH10 sample for NaYF₄:Yb³⁺, Tm³⁺ microcrystals under 980 nm excitation at a power > 500 μ W

correlated with the photoluminescence plots as shown in Fig. 4. And The photographs of $\text{NaYF}_4:\text{Yb}^{3+}, \text{Tm}^{3+}$ microcrystals of 5, 10, 15 and 20 mol% Li^+ doped concentrations with pH4 value under 980 nm excitation also can be seen in Fig. 7 We observe that the up-conversion luminescence of those sample have almost brightness with the naked eyes. In order to distinguish the exact difference in luminescence intensity of Li^+ doped concentrations samples, we need to view the up-conversion luminescence spectra.

Figure 8 shows the up-conversion luminescence spectra of $\text{NaYF}_4:\text{Yb}^{3+}, \text{Tm}^{3+}$ microcrystals of 0, 5, 10, 15 and 20 mol% Li^+ doped concentrations upon excitation with a 980 nm laser diode. Up-conversion luminescence intensities at 454 nm blue emission and that at 345 and 360 nm both violet emission which are caused by the transitions of $^1\text{I}_6 \rightarrow ^3\text{H}_5$ and $^1\text{D}_2 \rightarrow ^3\text{H}_6$, respectively. When the concentration of Li^+ varies from 5 to 20 mol%, the up-conversion emission intensities at both 345 and 360 nm also increase distinctly. The improved amplitude of up-conversion emission intensities which compared to the enhanced magnitude of 454 nm blue emission is different. The added degree of luminescence intensity with 454 nm blue emission is less than 345 and 360 nm violet emission. When the concentration of Li^+ enhances from 10 to 15 mol%, all of them have increasing rapidly. The contrast with their changes in luminescence intensity which displays the intensity of blue emission 479 nm is also increased when the concentration of Li^+ lifts up from 5 to 20 mol%. And the spacing of rapid increasing is in the concentration of Li^+ rises from 5 to 10 mol%. As for the luminescence intensity of IR emission at 796 nm, substantial increasing can be found with the interval of Li^+ concentration from 5 to 10 mol%. The intensity also decreased significantly when Li^+ concentration reach to 15 mol%.

When Li^+ concentration increases from 5 to 10 mol%, the transition system of up-conversion prone to get on the path of IR emission at 796 nm, which involves in fewer photon transitions. And then the concentration of Li^+ rises to 15 mol%. Multi-photon processes begin to dominate the system and make the luminescence intensity of blue and violet emission enhance.



Fig. 7 Photographs of UC luminescence of **a** 5% Li^+ concentrations sample, **b** 10% Li^+ concentrations sample, **c** 15% Li^+ concentrations sample, **d** 20% Li^+ concentrations sample for $\text{NaYF}_4:\text{Yb}^{3+}, \text{Tm}^{3+}$ microcrystals under 980 nm excitation at a power > 500 μW

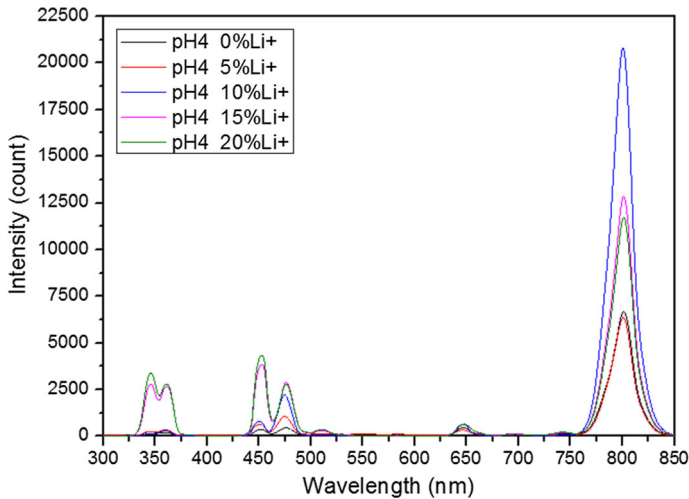


Fig. 8 UC luminescence spectra of NaYF₄:Yb³⁺, Tm³⁺ microcrystals doped with the Li⁺ concentrations of 0, 5, 10, 15 and 20 mol% under 980 nm excitation

The up-conversion luminescence intensities are improved by 3 and 8 times respectively with the blue emission 479 and 454 nm in NaYF₄:Yb³⁺, Tm³⁺ microcrystals via 20 mol% Li⁺ doping than that of Li⁺-free sample. Similarly the up-conversion luminescence of 345 and 360 nm are about 10 and 7 times than that of Li⁺-absent sample respectively. The most important reason for the strength of up-conversion emission intensity is that the Li⁺ doping can cause the distortion of local symmetry around rare-earth ions. The intensity of all emission peak were enhanced with the increasing of Li⁺ concentration, and meet the maximum at 20 mol% Li⁺. Li⁺ ions can diffuse into the interstitial positions of the host lattice NaYF₄: Yb³⁺, Tm³⁺ when lithium ions are doped. Thus, the local symmetry around Tm³⁺ is slightly influenced and brings about an increase in anti-Stokes luminescent phenomenon. Besides the adjustment of the local crystal field, doping Li⁺ ions also affects ETU (Energy Transfer Up-conversion) and processes of energy relaxation. The result can be concluded that up-conversion luminescence is improved by Li⁺ co-doping.

4 Conclusion

In summary, we successfully synthesized hexagonal NaYF₄:Yb³⁺, Tm³⁺ microcrystals used hydrothermal method with no impurities. The lower pH value measured in initial reaction solution made luminescent properties of up-conversion materials better, which is relative to the morphology of NaYF₄ microcrystals that are uniform hexagonal micro-prisms.

The distortion of the crystal symmetry around other rare-earth ions is caused by Li⁺ adjunction. Compared to Li⁺-free counterparts, higher concentration of Li⁺ has strong fluorescence properties and intensities. The blue emission 479 nm luminescence intensities and 454 nm luminescence intensities in NaYF₄:Yb³⁺, Tm³⁺ microparticles doped 20 mol% Li⁺ are enhanced 3 and 8 times, separately. Violet emission luminescence intensities around 345 and 360 nm are about 10 and 7 times, respectively.

From the results observed, we know the brightness of blue and violet emissions can be increased by Li^+ doping can obviously. The phenomenon explain that the enhanced up-conversion luminescence of $\text{NaYF}_4:\text{Yb}^{3+}, \text{Tm}^{3+}$ microparticles with Li^+ doped have the potentiality to be applied to many devices of convert light energy such as solar cells.

References

- Cao, T., Yang, T., Gao, Y., Yang, Y., Hu, H., Li, F.: Water-soluble $\text{NaYF}_4:\text{Yb}/\text{Er}$ upconversion nanophosphors: synthesis, characteristics and application in bioimaging. *Inorg. Chem. Commun.* **13**, 392–394 (2010)
- Chatti, M., Adusumalli, V.N., Ganguli, S., Mahalingam, V.: Near-infrared light triggered superior photocatalytic activity from $\text{MoS}_2\text{-NaYF}_4:\text{Yb}^{3+}/\text{Er}^{3+}$ nanocomposites. *Dalton Trans.* **45**, 12384–12392 (2016)
- Chen, H.Q., Yuan, F., Wang, S.Z., Xu, J., Zhang, Y.Y., Wang, L.: Near-infrared to near-infrared upconverting $\text{NaYF}_4:\text{Yb}^{3+}, \text{Tm}^{3+}$ nanoparticles-aptamer-Au nanorods light resonance energy transfer system for the detection of mercuric(II) ions in solution. *Analyst* **138**, 2392–2397 (2013)
- Chen, B., Sun, T., Qiao, X., Fan, X., Wang, F.: Directional light emission in a single NaYF_4 microcrystal via photon upconversion. *Adv. Opt. Mater.* **3**, 1577–1581 (2015)
- Cheng, L., Yang, K., Shao, M., Lee, S.-T., Liu, Z.: Multicolor in vivo imaging of upconversion nanoparticles with emissions tuned by luminescence resonance energy transfer. *J. Phys. Chem. C* **115**, 2686–2692 (2011)
- Chun-Long, X., Jin-Guo, W., Xiang-Yu, Z.: Strong single-band down-conversion emission in Tm^{3+} -doped NaYF_4 microparticles. *Acta Phys. Chim. Sin.* **31**, 2183–2190 (2015)
- Dou, Q., Zhang, Y.: Tuning of the structure and emission spectra of upconversion nanocrystals by alkali ion doping. *Langmuir* **27**, 13236–13241 (2011)
- Etchart, I., Hernández, I., Huijgnard, A., Bérard, M., Laroche, M., Gillin, W.P., Curry, R.J., Cheetham, A.K.: Oxide phosphors for light upconversion; Yb^{3+} and Tm^{3+} co-doped Y_2BaZnO_5 . *J. Appl. Phys.* **109**, 063104 (2011)
- Gauthier, N., Raccurt, O., Imbert, D., Mazzanti, M.: Efficient sensitization of Ln^{3+} -doped NaYF_4 nanocrystals with organic ligands. *J. Nanoparticle Res.* **15**, 1–14 (2013)
- Gnanasamandhan, M.K., Idris, N.M., Bansal, A., Huang, K., Zhang, Y.: Near-IR photoactivation using mesoporous silica-coated $\text{NaYF}_4:\text{Yb}, \text{Er}/\text{Tm}$ upconversion nanoparticles. *Nat. Protoc.* **11**, 688–713 (2016)
- Li, Z., Zhang, Y., Wu, X., Huang, L., Li, D., Fan, W., Han, G.: Direct aqueous-phase synthesis of sub-10 nm “luminous pearls” with enhanced in vivo renewable near-infrared persistent luminescence. *J. Am. Chem. Soc.* **137**, 5304–5307 (2015)
- Li, Z., Miao, H., Fu, Y., Liu, Y., Zhang, R., Tang, B.: Fabrication of $\text{NaYF}_4:\text{Yb}, \text{Er}$ nanoprobes for cell imaging directly by using the method of hydriol rivalry aided by ultrasonic. *Nanoscale Res. Lett.* **11**, 441 (2016)
- Li, H., Hao, S., Yang, C., Chen, G.: Synthesis of multicolor core/shell $\text{NaLuF}_4:\text{Yb}^{3+}/\text{Ln}^{3+}@\text{CaF}_2$ upconversion nanocrystals. *Nanomaterials (Basel)* **7**, 34 (2017)
- Liang, X., Wang, X., Zhuang, J., Peng, Q., Li, Y.: Synthesis of NaYF_4 nanocrystals with predictable phase and shape. *Adv. Funct. Mater.* **17**, 2757–2765 (2007)
- Lin, H., Xu, D., Teng, D., Yang, S., Zhang, Y.: Shape-controllable synthesis and enhanced upconversion luminescence of Li^+ doped $\beta\text{-NaLuF}_4:\text{Yb}^{3+}, \text{Ln}^{3+}$ ($\text{Ln} = \text{Tm}, \text{Ho}$) microcrystals. *New J. Chem.* **39**, 2565–2572 (2015a)
- Lin, H., Xu, D., Teng, D., Yang, S., Zhang, Y.: Simultaneous size and luminescence control of $\text{NaYF}_4:\text{Yb}^{3+}/\text{RE}^{3+}$ ($\text{RE} = \text{Tm}, \text{Ho}$) microcrystals via Li^+ doping. *Opt. Mater.* **45**, 229–234 (2015b)
- Liu, F., Ma, E., Chen, D., Yu, Y., Wang, Y.: Tunable red-green upconversion luminescence in novel transparent glass ceramics containing Er : NaYF_4 nanocrystals. *J. Phys. Chem. B* **110**, 20843–20846 (2006)
- Liu, Q., Feng, W., Yang, T., Yi, T., Li, F.: Upconversion luminescence imaging of cells and small animals. *Nat. Protoc.* **8**, 2033–2044 (2013)
- Liu, K.-C., Zhang, Z.-Y., Shan, C.-X., Feng, Z.-Q., Li, J.-S., Song, C.-L., Bao, Y.-N., Qi, X.-H., Dong, B.: A flexible and superhydrophobic upconversion-luminescence membrane as an ultrasensitive fluorescence sensor for single droplet detection. *Light Sci. Appl.* **5**, e16136 (2016a)

- Liu, L., Qin, F., Zhao, H., Lv, T., Zhang, Z., Cao, W.: Facile synthesis and upconversion luminescence of β -NaYF₄:Yb, Tm nanocrystals with highly tunable and uniform β -NaYF₄ shells. *J. Alloys Compd.* **684**, 211–216 (2016b)
- Nadort, A., Zhao, J., Goldys, E.M.: Lanthanide upconversion luminescence at the nanoscale: fundamentals and optical properties. *Nanoscale* **8**, 13099–13130 (2016)
- Page, R.H., Schaffers, K.I., Waide, P.A., Tassano, J.B., Payne, S.A., Krupke, W.F.: Upconversion-pumped luminescence efficiency of rare-earth-doped hosts sensitized with trivalent ytterbium. *J. Opt. Soc. Am. B* **15**, 996–1008 (1998)
- Pollnau, M., Gamelin, D.R., Lüthi, S.R., Güdel, H.U.: Power dependence of upconversion luminescence in lanthanide and transition-metal-ion systems. *Phys. Rev. B* **61**, 3337–3347 (2000)
- Schäfer, H., Ptacek, P., Eickmeier, H., Haase, M.: Synthesis of hexagonal Yb³⁺, Er³⁺-doped NaYF₄ nanocrystals at low temperature. *Adv. Funct. Mater.* **19**, 3091–3097 (2009)
- Shang, Y., Hao, S., Yang, C., Chen, G.: Enhancing solar cell efficiency using photon upconversion materials. *Nanomaterials (Basel)* **5**, 1782–1809 (2015)
- Shao, B., Feng, Y., Song, Y., Jiao, M., Lu, W., You, H.: Topotactic transformation route to monodisperse β -NaYF₄:Ln³⁺ microcrystals with luminescence properties. *Inorg. Chem.* **55**, 1912–1919 (2016)
- Suli, W., Ye, L., Jie, C., Yanhui, N., Shufen, Z.: β -NaYF₄:Yb³⁺, Er³⁺ upconversion microcrystals with both high emission intensity and controlled morphology. *Laser Photonics Rev.* **8**, 575–582 (2014)
- Timofeev, Y.P., Kirsanov, B.P., Than, N.K., Datskevich, E.I.: Cross-relaxational multiplication of electronic excitations of rare-earth ions. *J. Appl. Spectrosc.* **63**, 376–383 (1996)
- Wang, H.-Q., Nann, T.: Monodisperse upconverting nanocrystals by microwave-assisted synthesis. *ACS Nano* **3**, 3804–3808 (2009)
- Wang, G., Qin, W., Wang, L., Wei, G., Zhu, P., Kim, R.: Intense ultraviolet upconversion luminescence from hexagonal NaYF₄:Yb³⁺/Tm³⁺ microcrystals. *Opt. Soc. Am.* **16**, 11907–11914 (2008)
- Wang, M., Abbineni, G., Clevenger, A., Mao, C., Xu, S.: Upconversion nanoparticles: synthesis, surface modification and biological applications. *Nanomedicine* **7**, 710–729 (2011)
- Wang, K., Jiang, J., Wan, S., Zhai, J.: Upconversion enhancement of lanthanide-doped NaYF₄ for quantum dot-sensitized solar cells. *Electrochim. Acta* **155**, 357–363 (2015)
- Wu, S., Ning, Y., Chang, J., Niu, W., Zhang, S.: Modulation of the emission intensity and color output of NaYF₄: Yb³⁺, Er³⁺ nanocrystals by OH⁻. *CrystEngComm* **15**, 3919–3924 (2013)
- Wu, X., Chen, G., Shen, J., Li, Z., Zhang, Y., Han, G.: Upconversion nanoparticles: a versatile solution to multiscale biological imaging. *Bioconjug. Chem.* **26**, 166–175 (2015)
- Wu, R., Lei, L., Zhang, S., Xiao, Z., Zhang, J., Xu, S.: Promote the threshold of Tm³⁺ concentration using an inert-core/active-shell structure. *J. Mater. Chem. C* **4**, 9183–9186 (2016a)
- Wu, X., Tang, Z., Hu, S., Yan, H., Xi, Z., Liu, Y.: NaLuF₄:Yb³⁺, Er³⁺ bifunctional microcrystals codoped with Gd³⁺ or Dy³⁺ ions: enhanced upconversion luminescence and ferromagnetic-paramagnetic transition. *J. Alloys Compd.* **684**, 105–111 (2016b)
- Xiang, G., Zhang, J., Hao, Z., Zhang, X., Pan, G.-H., Luo, Y., Zhao, H.: Decrease in particle size and enhancement of upconversion emission through Y³⁺ ions doping in hexagonal NaLuF₄:Yb³⁺/Er³⁺ nanocrystals. *CrystEngComm* **17**, 3103–3109 (2015)
- Yang, M., Sui, Y., Wang, S., Wang, X., Sheng, Y., Zhang, Z., Lü, T., Liu, W.: Enhancement of upconversion emission in Y₃Al₅O₁₂:Er³⁺ induced by Li⁺ doping at interstitial sites. *Chem. Phys. Lett.* **492**, 40–43 (2010)
- Yi, G.S., Chow, G.M.: Synthesis of hexagonal-phase NaYF₄:Yb, Er and NaYF₄:Yb, Tm nanocrystals with efficient up-conversion fluorescence. *Adv. Funct. Mater.* **16**, 2324–2329 (2006)
- Yin, W., Zhao, L., Zhou, L., Gu, Z., Liu, X., Tian, G., Jin, S., Yan, L., Ren, W., Xing, G., Zhao, Y.: Enhanced red emission from GdF₃:Yb³⁺, Er³⁺ upconversion nanocrystals by Li⁺ doping and their application for bioimaging. *Chemistry* **18**, 9239–9245 (2012)
- Zhang, J., Hao, Z., Li, J., Zhang, X., Luo, Y., Pan, G.: Observation of efficient population of the red-emitting state from the green state by non-multiphonon relaxation in the Er³⁺-Yb³⁺ system. *Light Sci. Appl.* **4**, e239 (2015)
- Zhao, C., Kong, X., Liu, X., Tu, L., Wu, F., Zhang, Y., Liu, K., Zeng, Q., Zhang, H.: Li⁺ ion doping: an approach for improving the crystallinity and upconversion emissions of NaYF₄:Yb³⁺, Tm³⁺ nanoparticles. *Nanoscale* **5**, 8084–8089 (2013)
- Zhou, J., Liu, Z., Li, F.: Upconversion nanophosphors for small-animal imaging. *Chem. Soc. Rev.* **41**, 1323–1349 (2012)